

**Methods for permittivity, permeability, and loss measurements
of
polymer composite magneto-dielectric laminates**

Allen F. Horn III, Research Fellow – al.horn@rogerscorp.com
Christopher J. Caisse, R&D Engineer - chris.caisse@rogerscorp.com
Patricia A. LaFrance, Sr. Engineering Assistant - pat.lafrance@rogerscorp.com
Karl E. Sprentall, Business Development Manager – karl.sprentall@rogerscorp.com

Rogers Corporation
Advanced Connectivity Solutions – Lurie R&D Center
Rogers, CT USA

Abstract:

PTFE-ferrite composite laminates have recently been developed with nearly matched values of about 6.0 of electrical permittivity and magnetic permeability and low losses at frequencies of up to 500 MHz. These materials exhibit a large miniaturization factor ($\sqrt{\mu_R \epsilon_R}$) and impedance nearly matched to free space. These properties allow the design of smaller, lower profile antennas with significantly wider bandwidths and efficiencies. However, special test methods are required to independently measure the permittivity, permeability, and loss values.

Summary:

It has been well known for more than 50 years to use high dielectric constant copper clad laminates to reduce the size of wavelength dependent microstrip structures such as patch antennas.

In the general case, the material's impedance is $\sqrt{\mu_R/\epsilon_R} \sqrt{\mu_0/\epsilon_0}$ where μ_R and ϵ_R are the relative permeability and permittivity, respectively, and the subscript 0 values are those of free space. The miniaturization factor (by which the material decreases the wavelength of an EM signal) is $\sqrt{\mu_R \epsilon_R}$. While all natural solid materials exhibit an ϵ_R value > 1 , most materials are non-magnetic, with a $\mu_R = 1.0$. Thus, the high dielectric constant results in a material impedance significantly lower than free-space and a reduction in both bandwidth and antenna efficiency of microstrip patch antennas.

A recently developed PTFE – ferrite powder composite laminate exhibits $\mu_R \sim \epsilon_R \sim 6$ and low electrical and magnetic loss values at frequencies up to 500 MHz. This material has a miniaturization factor of a dielectric material with permittivity of 36, but with an impedance essentially matched to free space. Accurately measuring the permittivity, permeability, and loss values, however, presents challenges.

In the present work, we compare data from widely different test methods, including the Keysight Impedance Analyzer with 16453A and 16454A permittivity and permeability fixtures, coaxial airline perturbation, "full sheet resonance," and phase length, insertion loss and impedance of microstrip transmission lines over a frequency range of 40 MHz to 4 GHz. We explain the causes of both random measurement error and systematic error in the various test methods. Variation between test method results is often due to the anisotropy of the in-plane and z-axis permittivity and permeability and differences in the relative orientation of the electrical and magnetic fields in the test fixtures. Correctly modeling an antenna utilizing these recently developed materials requires an understanding of the anisotropy of these materials and the orientations of the electrical and magnetic fields in the antenna. In spite of requiring exacting sample preparation, the 25 mm coaxial airline yields the most reproducible data. Measured performance of transmission lines and antennas shows good agreement with Sonnet Software models using the measured values of permittivity and permeability.

Polymer ferrite composites:

Ferrimagnetic materials have been used for many years in a number of high frequency devices including circulators, isolators, gyrators and phase shifters¹. Historically the most widely used materials have been ferrite ceramics. Ferrites are mixed metal oxides with a wide range of composition doped garnets, Ni-Zn spinels, and barium cobalt Co₂Z hexaferrites. High loss polymeric composites comprising ferrite powders also have a long history in radar absorbing and cavity resonance reduction applications².

Since starting about 10 years ago, a number of researchers have investigated the feasibility and utility of $\mu_R \sim \epsilon_R$ polymer composites for antenna applications³⁻⁹. With a composite system of 45 volume% Co₂Z hexaferrite in polyethylene, Bo and Halloran³ achieved a $\mu_R = 3.5$ and $\epsilon_R = 8.0$ at 500 MHz. Park et al⁶, using 40 weight % Ni-Zn ferrite in a silicone elastomer, achieved $\mu_R = 2.2$ and $\epsilon_R = 3.8$ at 500 MHz. Tzanidis et al⁵ did not exceed a μ_R / ϵ_R ratio of greater than $\frac{1}{2}$ with several different types of ferrite, including Co₂Z. McKinzie and Rogers⁴ made a 50 weight % carbonyl Fe-filled isoprene composite with $\mu_R = 4.6$ and $\epsilon_R = 11.0$ and Raj et al used 25 volume% passivated nano-cobalt in a fluoropolymer to make a composite with $\mu_R = 1.9$ and $\epsilon_R = 7.4$. Martin et al⁹ obtained 500 MHz values of $\mu_R = 2.8$ and $\epsilon_R = 6.0$ with a 40 volume % BaCo ferrite in Sylgard 184 silicone elastomer, similar to the $\mu_R = 3.0$ and $\epsilon_R = 6.0$ at 300 MHz for a polymer ferrite composite described by Reese and Auckland and Reese⁷.

Polymer composite copper-clad laminates have been commonly used in high frequency systems for longer than 50 years. These materials are linear (unaffected by field strength), low dielectric loss composites with dielectric constant (permittivity) values ranging from 2 to about 13 and a magnetic permeability of 1.0. Over the frequency range of megahertz to terahertz, the change in dielectric constant with frequency (dispersion) is due to dipole rotation and electron cloud polarization and is governed by Debye relaxation with a wide range of relaxation times. For low loss materials, the dispersion is low, typically a 1 to 2% decrease in permittivity for each decade increase in frequency. Dielectric loss can either increase or decrease moderately with frequency, depending on the composition.

The frequency dependence of the real and imaginary parts of permeability, μ' and μ'' , is more complicated for ferrite and polymer-ferrite composites (Figure 1). μ' is generally constant up to

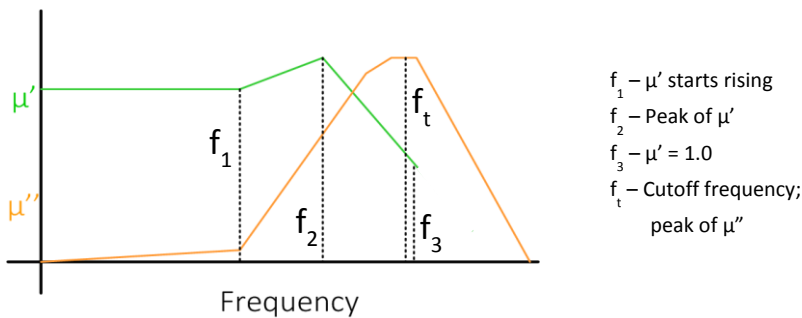


Figure 1
Typical μ' and μ'' behavior versus frequency

some frequency, f_1 , where it begins to increase as does μ'' also. μ' reaches a maximum value at the resonant frequency, f_2 , and then decreases. At f_3 , μ' reaches a value of 1.0. The frequency at which μ'' reaches its peak is defined as the cutoff frequency, f_c .

In order to achieve a $\mu_R = \epsilon_R$ low loss composite material, one must be operating the device at a frequency lower than the cut-off frequency, and preferably below f_1 , where μ' is stable with frequency and the μ'' is low. Co_2Z hexaferrites are predicted to have higher values of cut-off frequency than cubic materials such as spinels and garnets and have been the subject of considerable academic and industrial research^{2,6,9,11,12}. Current research comprises different dopants and processing conditions to achieve higher cut-off frequencies. As illustrated in the Skyworks Data Sheet figures for TTZ-100 and TTZ-500 hexagonal ferrites¹², higher cut-off frequency generally results in a lower permeability (figure 2).

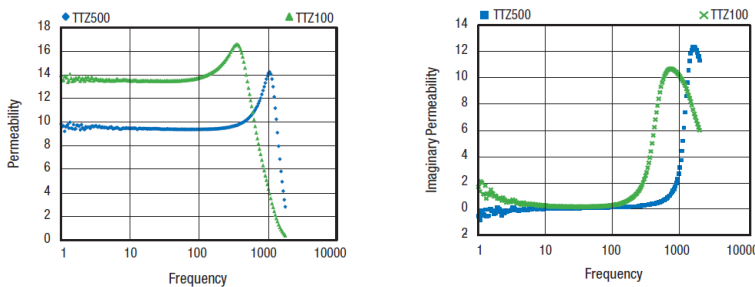


Figure 2
 μ' and μ'' for Skyworks TTZ-100 and TTZ-500 Hexaferrites – taken from reference 12
 Frequency in MHz

Rogers Corporation has recently introduced ferrite-filled PTFE composite material with an approximate $\mu_R = \epsilon_R = 6$, electric $\tan(\delta) < 0.005$, and magnetic $\tan(\delta) < 0.05$ at 400 MHz. Sold under the trade name of MAGTRES™ 555 high impedance laminate, the material may be copper foil clad for fabrication by traditional PCB methods or unclad for use as an antenna load. The material yields an effective substrate dielectric constant for miniaturization, $\mu_R \epsilon_R$ of 26 to 30, while exhibiting an impedance matched to free space. Use of MAGTRES 555 high impedance laminate can result in significant antenna size reduction without decreasing bandwidth. It is designed for use at frequencies of up to about 500 MHz. The panel size is 12"X18" with standard thickness values from 0.020" to 0.250" (0.5 to 6.25 mm).

Accuracy of dielectric constant values are key to system designers and repeatability is key to stable manufacturing of high frequency devices. Fairly early in the commercial history of copper-clad composite laminates for high frequency applications, the manufacturers agreed upon a clamped stripline resonator test fixture designed to resonate at x-band¹³. The test utilizes fully etched samples and the values do not depend on precise knowledge of the sample thickness. The fact that it is a loosely coupled resonator removes the necessity of accurate calibration to obtain consistent results.

Figure 3: IPC-TM-650 2.5.5.5C clamped stripline test fixture. The two 1.5 mm fully etched coupons are inserted on either side of the patterned resonator card and the fixture is closed to form a stripline circuit



Fully etched samples are placed on either side of the resonator card and closed under tightly controlled force and a frequency sweep is run with a network analyzer. The ϵ_R is calculated as

$$\epsilon_R = (n c / 2 f_r (L + \Delta L))^2 \quad (1)$$

where n is the peak node number, c is the speed of light, f_r is the peak resonant frequency, L is the resonator length, and ΔL is the correction for fringing capacitance which is close in value to the dielectric thickness, as discussed in detail in the test method¹³. The results have been found to be operator independent and precise and accurate. For low dielectric constant materials the 95% confidence limit for permittivity approaches +/- 0.005¹⁴.

Being able to effectively design an electromagnetic device with a material with both $\epsilon_R \gg 1$ and $\mu_R \gg 1$ requires knowledge of ϵ_R and μ_R independently, along with the associated dielectric and magnetic losses. These constitute four “unknowns,” ϵ' , μ' , ϵ'' , and μ'' .

Most high frequency permeability and permittivity tests consist of a “device under test” (DUT) containing the “material under test” (MUT) in such a way that it is easy to extract the dielectric and magnetic properties from the performance of the DUT.

A two-port vector network analyzer (VNA) measures the phase and magnitude (power level) of the four S parameters: S_{11} – signal sent from port 1 that is reflected to port 1, S_{21} – signal sent from port 1 that is transmitted to port 2, S_{22} – signal sent from port 2 that is reflected to port 2, and S_{12} – signal sent from port 2 that is transmitted to port 1.

The magnitude and phase of the reflected signals, S_{11} and S_{22} , depend on the impedance within the DUT, which in turn depends upon the geometry of the DUT and MUT and the impedance of the MUT, $\sqrt{\mu_R / \epsilon_R}$.

The magnitude and phase of the transmitted signals, S_{21} and S_{12} , depend on the miniaturization factor, $\sqrt{\mu_R \epsilon_R}$ and the magnetic and dielectric losses of the MUT.

Transmission lines are widely used as test fixture DUTs. These can include waveguides, coaxial air lines, and microstrip and stripline circuits. There are several ways of using transmission lines to extract material properties. One method is to create a resonator by imposing impedance discontinuities such as the gap between the probe lines in the clamped stripline resonator (figure 1), placing a capacitively coupled ring in a microstrip transmission line (figure 4a) or the iris plates at each end of a waveguide cavity resonator (figure 4b).

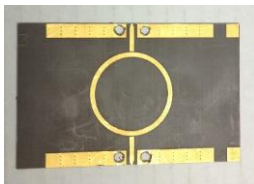


Figure 4a – microstrip ring resonator

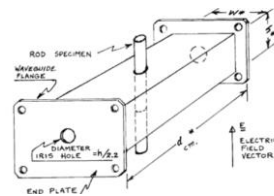


Figure 4b – waveguide cavity resonator

In the case of the clamped stripline resonator with a material with both $\epsilon_R \gg 1$ and $\mu_R \gg 1$, the miniaturization factor is calculated analogous to equation 1.

$$\sqrt{\mu_R \epsilon_R} = (n c / 2 f_r (L + \Delta L))^2 \quad (2)$$

In the case of the microstrip ring resonator, an “effective miniaturization factor” for the microstrip assembly will be obtained

$$\sqrt{\mu_R \epsilon_R}^{\text{eff}} = (n c / f_r 2\pi R)^2 \quad (3)$$

and further modeling with electromagnetic simulation software will be necessary to extract the $\sqrt{\mu_R \epsilon_R}$ value of the material itself.

In the case of the waveguide resonant cavity, the resonant frequency and Q is measured for the empty cavity. A small sample of the material which can be any of a wide variety of shapes is placed at the centerline of the cavity (figure 4b) and the resonant frequency and Q of the “perturbed” (sample-loaded) cavity is measured. The miniaturization factor is calculated from the resonant frequency change, sample shape and dimensions described in reference 15 and the loss values are calculated from the change in cavity Q.

If the resonant structure is “loosely coupled” (with the resonant peak 20 dB down or more), then frequency calibration of the cables and fixture are not necessary. However, since the impedance discontinuity, such as the gap in the probe line (figs. 1 & 4a) or iris plates (figure 4b) is external to the MUT, one is not able to measure the impedance of the material itself.

With a resonant transmission line test, the ϵ_R and μ_R values cannot be obtained separately and only the overall miniaturization factor, $\sqrt{\mu_R \epsilon_R}$, can be measured.

Transmission/Reflection Methods

Baker-Jarvis et al¹⁵ from NIST-Boulder describe non-resonant transmission line test methods using waveguides and coaxial airlines. These test methods are designed to have the MUT be the major influence on both reflection and transmission so μ_R , ϵ_R , and the dielectric and magnetic loss values can be independently obtained. Since we expect most applications for the MAGTRES 555 laminate to be in the range of 100 MHz to 700 MHz or so, we are most interested in μ_R and ϵ_R data over that frequency range. At such low frequencies, waveguides would be very large and several bands would be required to cover the desired frequency range. The coaxial airline is inherently broad band. Standard OD’s of airlines are 7 mm, 14, and 25 mm.

The airline test consists of calibration of the fixture with a short and several lengths of “through” TLs. The “automatic fixture removal” (AFR) built into the Keysight PLTS materials measurement software system. A sample consists of an annular ring of the MUT with good planarity and precisely machined ID and OD to fit the inner and outer conductors of the coaxial airline. The full S-parameters are measured and analyzed using the Nicholson-Weir-Ross algorithm discussed in detail in reference 16.

Based on an informal survey of the literature, the 7 mm and 14 mm diameter airlines appear to be preferred, probably due to the small sample size required. However, a subsequent “round robin” test of 7 mm and 14 mm airlines by NIST¹⁷ showed that the major source of error was the precision of machining and accounting for the air gaps between the sample and inner and outer conductors, if they existed, in the analysis. This primarily affected the permittivity values and the effect decreased with the larger diameter airline. In order to achieve the best reproducibility, we chose a 25 mm diameter clam-shell airline manufacture by Damaskos, Inc. of Concordville, PA (Figure 5). Typical data are shown from 100 MHz to 3 GHz in Figure 6.



Figure 5
 Damaskos Inc., 25 mm Clamshell Airline (open) with sample at centerline

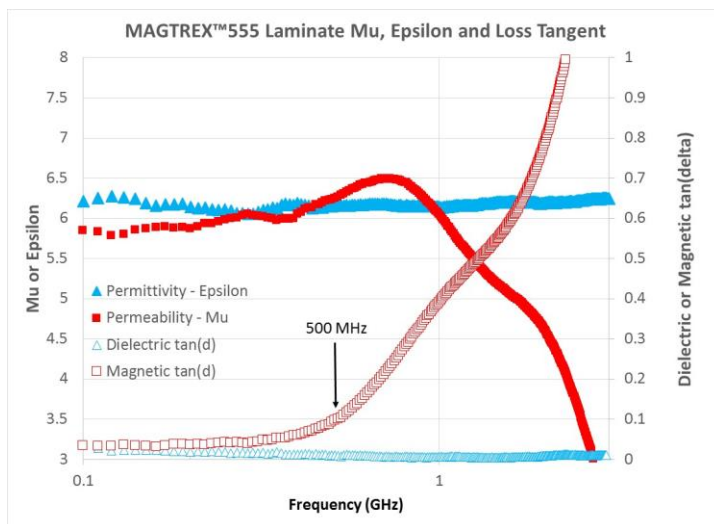


Figure 6
 Typical μ_R , ϵ_R , and electrical and magnetic $\tan(\delta)$ data from 100 MHz to 3.0 GHz

Composite Mixing Rules and Anisotropy

As described by Neelakanta¹⁸, the mixing rules that predict the properties of a composite, such as permeability, permittivity, thermal conductivity, or modulus, based on those of its components depend highly on the spatial arrangement of the components, as well as the volume fraction of each component.

The parallel arrangement of materials (figure 7a) leads to a simple mixing rule in which the composite property is the sum of the component properties weighted for their volume fraction in the composite. In the case of the ϵ_r of a composite with N components

$$\epsilon_{Rcomposite} = \sum_{i=1}^N v_i \epsilon_{Ri} \quad (4)$$

where v_i is the volume fraction of component i and ϵ_{Ri} is the permittivity of that component. The parallel arrangement is the upper bound for ϵ_r , as well as dielectric constant and modulus. The parallel arrangement is a reasonable model for the in-plane properties of woven glass fabric reinforced resin composites like epoxy-glass FR4 laminate or woven glass-PTFE high frequency laminate.

The series arrangement (figure 7b) leads to the lower bound for a composite's thermal conductivity, permittivity, and modulus. The ϵ_r of a series composite is given by

$$\epsilon_{Rcomposite} = 1 / \sum_{i=1}^N v_i \epsilon_{Ri}^{-1} \quad (5)$$

The z-axis (through plane) properties of resin impregnated woven glass fabric composites are examples of composite material properties that are very nearly approximated by the series model.

Over the years, a number of models of varying degrees of complexity have been proposed to describe the behavior of dispersed phase composites (figure 13c). A major consideration is accounting for the proportion of series and parallel character of each phase. Obviously, the continuous phase exhibits some degree of parallel character due to its continuity. A convenient equation that often yields remarkably good agreement given its simplicity is the logarithmic mixture law¹³ also known as Lichtenecker's rule given by

$$\log(\epsilon_{Rcomposite}) = \sum_{i=1}^N v_i \log(\epsilon_{Ri}) \quad (6)$$

A dispersed phase composite is an approximation of a ceramic powder filled polymeric material. The logarithmic mixing rule predicts an isotropic permittivity which is, in fact observed, if the dispersed filler particles are spherical.

However, with irregularly shaped filler particles, the sheet forming process selectively aligns the particles, resulting in surprisingly high values of anisotropy. In particular, by their crystalline nature, the hexaferrite particles are platelets that align easily, giving a more highly parallel structure in-plane, leading to higher in-plane value of permittivity and permeability than through the z-axis (figure 8).

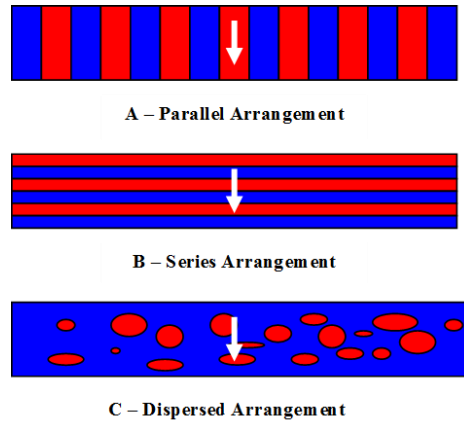


Figure 7
Composite material component geometries

In the most general case, the permittivity of an anisotropic material will be described by a nine element tensor.

$$\begin{pmatrix} D_x \\ D_y \\ D_z \end{pmatrix} = \begin{pmatrix} \epsilon_{xx} & \epsilon_{xy} & \epsilon_{xz} \\ \epsilon_{yx} & \epsilon_{yy} & \epsilon_{yz} \\ \epsilon_{zx} & \epsilon_{zy} & \epsilon_{zz} \end{pmatrix} \begin{pmatrix} E_x \\ E_y \\ E_z \end{pmatrix} \quad (7)$$

However, as a practical matter, the off-diagonal elements such as ϵ_{xy} (quantifying the displacement flux in the x direction arising from the electric field in the y-direction) are insignificant in common dielectric materials and it is sufficient to only consider the diagonal elements

$$\begin{pmatrix} D_x \\ D_y \\ D_z \end{pmatrix} = \begin{pmatrix} \epsilon_{xx} & 0 & 0 \\ 0 & \epsilon_{yy} & 0 \\ 0 & 0 & \epsilon_{zz} \end{pmatrix} \begin{pmatrix} E_x \\ E_y \\ E_z \end{pmatrix} \quad (8)$$

Furthermore, in circuit laminates, ϵ_{xx} and ϵ_{yy} rarely differ significantly from each other and for modeling purposes, only the z-axis (out of plane) value, ϵ_{zz} , and x-y plane (in-plane) value, ϵ_{x-y} are used. The coaxial airline, by nature, measures the in-plane average permittivity and permeability, ϵ_{x-y} , and cannot resolve the individual components, ϵ_{xx} and ϵ_{yy} .

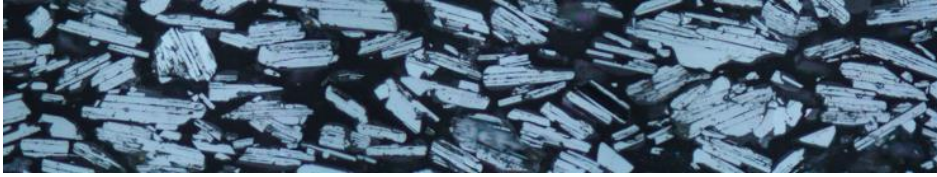


Figure 8
SEM of cross section of Magtrex™555 High Impedance Laminate

ϵ_R and μ_R Anisotropy by different test methods

Different types of transmission lines will support different electromagnetic field configurations. A comparison of the EM fields (figure 9) shows that the TEM mode in the coaxial airline has both the magnetic and electric fields oriented in-plane to the MUT, while the TEM mode in the parallel plate waveguide and quasi-TEM mode in microstrip have the magnetic field predominantly in-plane and the electric field out-of-plane.

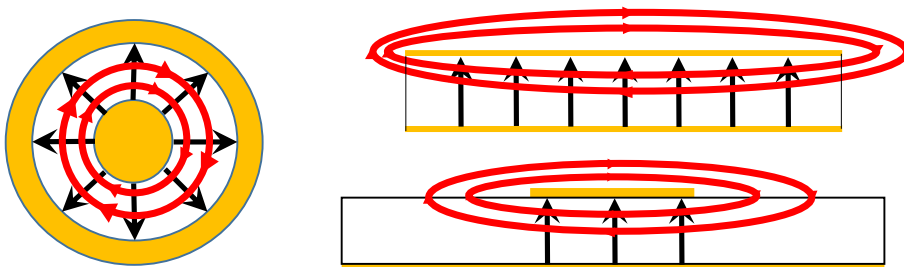


Figure 9
Electric (black) and magnetic (red) field orientations in TEM for coaxial cable, parallel plate waveguide and microstrip configurations.

A copper-clad laminate itself can function as a dielectric-filled parallel plate waveguide, providing a method for a non-destructive measurement of dielectric properties^{19,20}. The cable connection to the laminate creates a large impedance discontinuity, so the laminate acts as a resonator, so one is not able to calculate μ_R and ϵ_R independently. The test method is known as “full sheet resonance.” While the test methods described in references 19 and 20 envision a non-magnetic medium, the derivation by Pozar²¹ shows that the miniaturization factor will be $\mu_R \epsilon_R$ for a parallel plate waveguide, so this can be applied to the FSR test.

A frequency sweep is conducted and the resonant peaks are identified. The $\mu_R \epsilon_R$ product is calculated as

$$\mu_R \epsilon_R = \left(\frac{c}{2f_{R[M:N]}} \right)^2 \left(\left\{ \frac{M}{L} \right\}^2 + \left\{ \frac{N}{W} \right\}^2 \right) \quad (9)$$

Where c is the speed of light, $f_{R[M:N]}$ is the resonant frequency of mode $M:N$, and L and W are the length and width of the panel. While not reflected in this basic equation, the calculated $\mu_R \epsilon_R$ product does change with panel size and thickness due to non-ideal conductor effects and fringing capacitance at the panel edges. The calculated value increases with decreasing panel thickness. One hundred mil thick panels exhibit an FSR $\mu_R \epsilon_R$ product of about 25 in 0.100" laminates and values of 26 to 30 in thinner materials. With a 12"x18" panel of magnetodielectric material, the lower order mode frequencies will be at quite low values. $F_{R(1:0)}$ and $F_{R(2:0)}$ occur at approximately 60 and 120 MHz, respectively.

The $\mu_R \epsilon_R$ product from the airline data is about 36. The FSR value is lower due to the material's anisotropy of μ_R and ϵ_R and the different electric and magnetic field orientations in the two tests. The more highly parallel nature of the filler orientation in-plane contributes to a higher in-plane ϵ_R and μ_R value. In the coaxial airline test, both the electric and magnetic fields are in-plane. However, with the FSR configuration, the electric field is purely out-of-plane and the magnetic field is pure in plane. If we assume that the effective in-plane μ_R of about 6.0 measured by airline is unchanged in the FSR configuration, the $\mu_R \epsilon_R$ product of about 30 in thin laminates would imply a z-axis ϵ_R of about 5.0

To validate the utility of our extracted values μ_R and ϵ_R in modeling, we used Sonnet Software and fixed values of $\epsilon_R = 5.0$ and $\mu_R = 6.0$ to estimate microstrip 50 ohm transmission lines widths of 0.042", 0.080", and 0.112" on 0.010", 0.020" and 0.030" laminates at about 500 MHz. These were fabricated and tested from 100 MHz to 3 GHz using long and short circuits to generate phase length and insertion loss data. Note that we intentionally measured far beyond the expected useful low loss frequency maximum of about 500 MHz, to test the validity of our data up to 3 GHz.

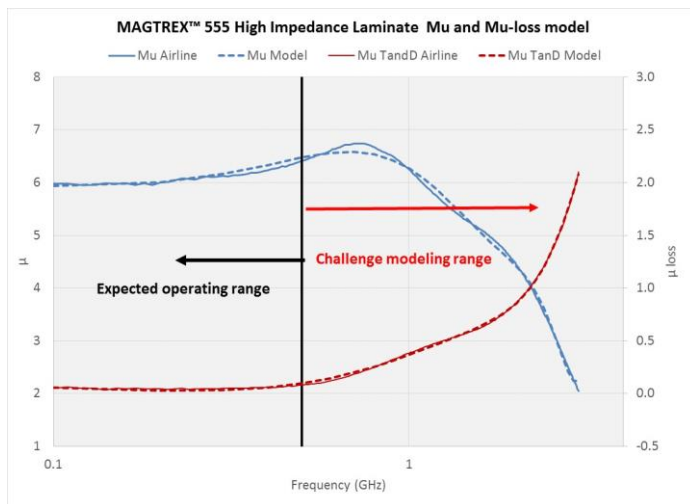


Figure 10
Measured and polynomial fit values of freq. dependent μ and magnetic loss

Recall permeability and magnetic loss are quite sensitive to frequency while permittivity and dielectric loss are not. For an accurate test of our data we chose to fit a six term polynomial to the permeability data and fifth term polynomial to the magnetic loss data from 100MHz to 3 GHz. While the

expected use range as a low loss magneto-dielectric is below 500- 700MHz or so, we chose to also model the challenging higher frequencies where significant changes occur to test our broad band measurement validity (figure 10). While using the frequency dependent permeability and magnetic loss data, we used a fixed value of $\epsilon_R = 5.0$ and dielectric $\tan\delta = 0.005$.

The fitted magnetic permeability and loss values, constant dielectric constant of 5.0 and loss value of 0.005 and measured circuit dimensions were used in Sonnet Software to model the K'_{eff} of the three thicknesses of microstrip circuits and insertion loss. They show very good agreement with the measured values at all three thicknesses of laminate (figure 11 and 12).

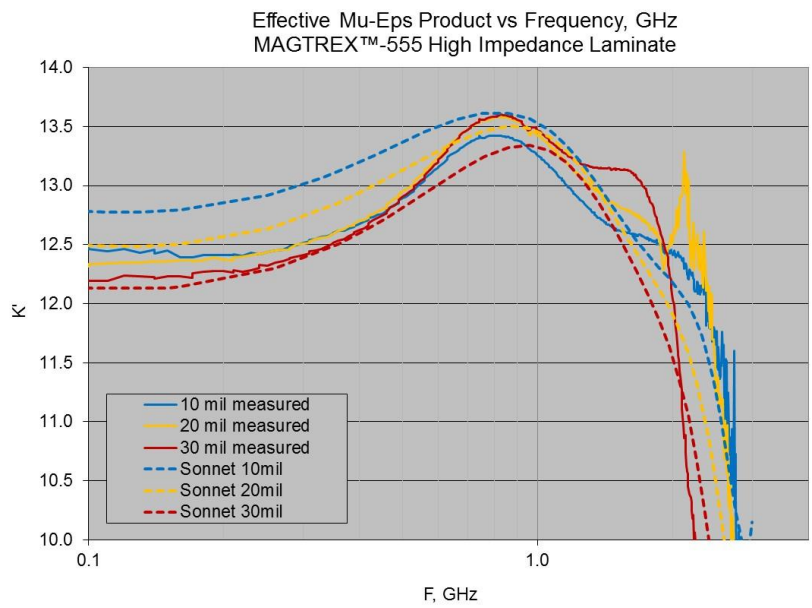


Figure 11

Measured and Sonnet Modeled Effective $\mu_R \epsilon_R$ of 50 ohm TLs on 10, 20, and 30 mil laminates
Measurements were made at frequencies higher than the expected use range to
demonstrate broad band validity.

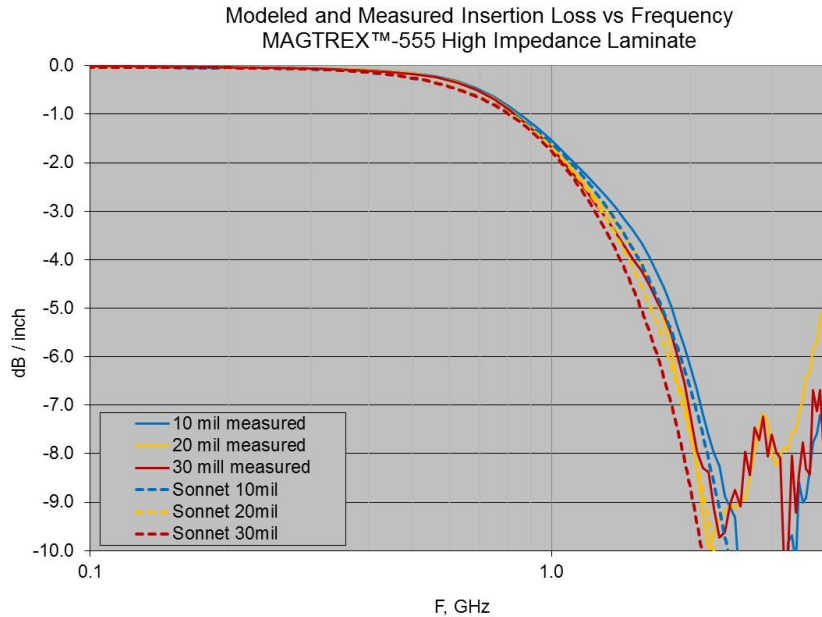


Figure 12
Measured and Sonnet Modeled Insertion loss of 50 ohm TLs on 10, 20, and 30 mil laminates
Measurements were made at frequencies higher than the expected use range to
demonstrate broad band validity.
Note that even the details of the curves above 2 GHz are accurately modeled.

Impedance Analyzer Measurements

The Keysight 16453A Dielectric Test Fixture and 16454A Magnetic Material Test fixture are frequently used with the 4990A Impedance analyzer for permittivity and permeability measurements up to 1 GHz. However, the operating manual²² clearly states that, irrespective of sample size, with sample permeability in the range of 3 to 10, one should be anticipating greater than 10% error and increasing with frequency above 200 MHz.

We tested an experimental magneto-dielectric material by the three test methods. A comparison (figure 13) of coaxial airline and Keysight16454A results from 100 MHz to 1 GHz, indeed show an increasing systematic error in the permeability meter data above 400 GHz.

The dielectric test fixture (figure 14) also incorrectly shows permittivity increasing with frequency and a 5-10 % higher value than the airline data.

These fixtures are not appropriate for measuring materials with moderate permittivity and permeability values in the 100 MHz to 1 GHz frequency range.

Commented [AFH1]:

Commented [AFH2R1]:

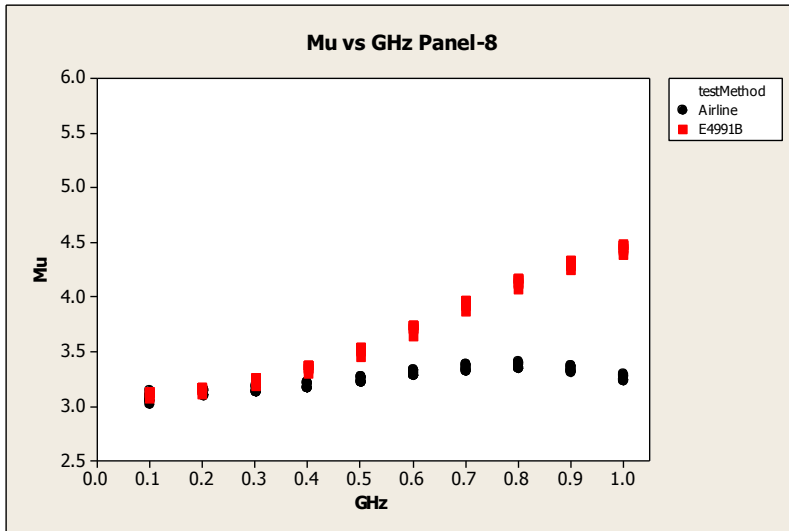


Figure 13
 Systematic discrepancy between coaxial airline and impedance analyzer permeability increases at frequencies of 400 MHz . The discrepancy is nearly 40% at 1 GHz.
 Data taken on an experimental magneto-dielectric composite.

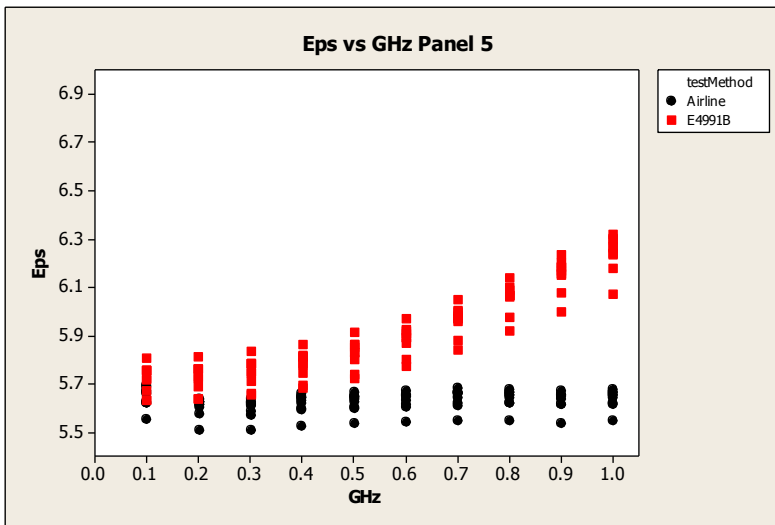


Figure 14
 Systematic permittivity discrepancy between coaxial airline and impedance analyzer data
 Permittivity does not increase with frequency. The discrepancy is nearly 10% at 1 GHz.
 Data taken on an experimental magneto-dielectric composite.

Conclusion

Accurate and repeatable measurement of the permittivity and permeability of polymer magneto-dielectric composites presents special challenges. With a combination of 25 mm coaxial airline and full sheet resonance testing, we are able to extract data that result in accurate modeling of simple circuit performance.

References

1. D. M. Pozar, Microwave Engineering, pp. 497-542, 2nd edition, J. Wiley & Sons, 1998
2. P. Dixon, *Theory and application of microwave/RF absorbers*, Emerson and Cumming Tech Notes, www.eccosorb.com
3. T. B. Do and J. W. Halloran, *Fabrication of Polymer Magnetics*, IEEE Antenna and Propagation Society International Symposium, pp. 1709-1712, July 2007
4. W. E. McKinzie III & S. D. Rogers, *Experimental results of an AMC antenna fabricated with a magnetically loaded elastomeric substrate*, IEEE International Antenna and Propagation Symposium, San Diego, CA, July 5-12, 2008
5. I. Tzanidis, S. Koulouridis, K. Sertel, D. Hansford and J. L. Volakis, *Characterization of Low-loss Magnetodielectric Composites for Antenna Size Reduction*, IEEE International Antenna and Propagation Symposium, San Diego, CA, July 5-12, 2008
6. S. Park, W. Ahn, J. Kum, J. Ji, K. Kim, and W. Seong, *Electromagnetic Properties of Dielectric and Magnetic Composite Material for Antenna*, Electronic Materials Letters, Vol. 5, No. 2, pp. 67-71 (2009)
7. D. T. Aukland & M. Reese, *A conformal UHF antenna suitable for satellite communications by small air, land, and sea sensor platforms*, IEEE 2011 Military Communications Conference Proceedings, pp. 1808-1811, 2011
8. P. M. Raj, H. Sharma, G. P. Reddy, D. Reid, N. Altunyurt, R. Tummala, and V. J. Nair, *Novel Nanomagnetic Materials for High-Frequency RF Applications*, IEEE 2011 Electronic Components and Technology Conference, Lake Buena Vista, FL, June 2011
9. L. Martin, D. Staiculescu, L. Yang, *Flexible Magnetic Composites*, Chapter 8 in Passive RF Component Technology, G. Wang & B. Pan, Eds., Artech House, December 31, 2011
10. A. von Hippel, editor, Dielectric Materials and Applications, J. Wiley and Sons, NY, 1954
11. L. Zhang, A. Puri, K. Sertel, J. L. Volakis, and H. Verweij, *Low Loss Z-Type Ba₃Co₂Fe₂₄O₄₁ Hexaferrites for Antennas and RF Devices*, IEEE Trans. on Magnetics, vol. 47, no. 8, August 2011
12. Skyworks Data Sheet: TTZ-100 and TTZ-500 hexagonal ferrites, www.skyworksinc.com, 2017
13. IPC-TM-650 2.5.5.5C, *Stripline Test for Permittivity and Loss Tangent (Dielectric Constant and Dissipation Factor) at X-Band*, www.ipc.org, March 1998
14. A. F. Horn, III, P. A. LaFrance, J. W. Reynolds, J. Coonrod, *The influence of test method, conductor profile, and substrate anisotropy on the permittivity values required for accurate modeling of high frequency planar circuits*, Circuit World, v.38, n.4, pp. 219-231, 2012
15. ASTM D2520-13, *Standard Test Methods for Complex Permittivity (Dielectric Constant) of Solid Electrical Insulating Materials at Microwave Frequencies and Temperatures to 1650°C*
16. J. Baker-Jarvis, M. J. Janezic, J. H. Grosvenor, Jr., R. G. Geyer, *Transmission/Reflection and Short-Circuit Line Methods for Measuring Permittivity and Permeability*, NIST Technical Note 13555, May 1992
17. C. M. Weil, M. J. Janezic, E. J. Vanzura, *Intercomparison of Permeability and Permittivity Measurements using the Transmission/Reflection Method in 7 and 14 mm Coaxial Airlines*, NIST Technical Note 1386, March 1997
18. Neelakanta, P. S., *Handbook of Electromagnetic Materials*, pp. 108-111, CRC Press, New York (1995)
19. R. L. Lewis, *Relative Permittivity Measurement of Square Copper-Laminated Substrates using the Full-Sheet Resonance Method*, NISTIR 5053, January 1997
20. IPC-TM-650 2.5.5.6, *Non-Destructive Full Sheet Resonance Test for Permittivity of Clad Laminates*, May 1989
21. D. M. Pozar, Microwave Engineering, pp. 112-120, 2nd edition, J. Wiley & Sons, 1998
22. Agilent 16454A Magnetic Material Test Fixture: Operation and Service Manual, July 2001